ORIGINAL ARTICLE

Positive End-Expiratory Pressure Ventilation Induces Longitudinal Atrophy in Diaphragm Fibers

Johan Lindqvist[1]*, Marloes van den Berg[2]*, Robbert van der Pijl[1,2], Pleuni E. Hooijman[2], Albertus Beishuizen[3], Judith Elshof[4], Monique de Waard[4], Armand Girbes[4], Angelique Spoelstra-de Man[4], Zhong-Hua Shi[5], Charissa van den Brom[6], Sylvia Bogaards[2], Shengyi Shen[1], Joshua Strom[1], Henk Granzier[1], Jeroen Kole[2], René J. P. Musters[2], Marinus A. Paul[7], Leo M. A. Heunks[4], and Coen A. C. Ottenheijm[1,2]

[1]Cellular and Molecular Medicine, University of Arizona, Tucson, Arizona; [2]Department of Physiology, [4]Department of Intensive Care, [6]Department of Anesthesiology, and [7]Department of Cardiothoracic Surgery, Vrije Universiteit Medical Center, Amsterdam, the Netherlands; [3]Department of Intensive Care, Medisch Spectrum Twente, Enschede, the Netherlands; and [5]Department of Critical Care Medicine, Beijing Tiantan Hospital, Capital Medical University, Beijing, PR China

ORCID IDs: 0000-0003-4010-013X (J.L.); 0000-0003-0920-6139 (M.v.d.B.).

Abstract

Rationale: Diaphragm weakness in critically ill patients prolongs ventilator dependency and duration of hospital stay and increases mortality and healthcare costs. The mechanisms underlying diaphragm weakness include cross-sectional fiber atrophy and contractile protein dysfunction, but whether additional mechanisms are at play is unknown.

Objectives: To test the hypothesis that mechanical ventilation with positive end-expiratory pressure (PEEP) induces longitudinal atrophy by displacing the diaphragm in the caudal direction and reducing the length of fibers.

Methods: We studied structure and function of diaphragm fibers of mechanically ventilated critically ill patients and mechanically ventilated rats with normal and increased titin compliance.

Measurements and Main Results: PEEP causes a caudal movement of the diaphragm, both in critically ill patients and in rats, and this caudal movement reduces fiber length. Diaphragm fibers of 18-hour mechanically ventilated rats (PEEP of 2.5 cm H_2O) adapt to the reduced length by absorbing serially linked sarcomeres, the smallest contractile units in muscle (i.e., longitudinal atrophy). Increasing the compliance of titin molecules reduces longitudinal atrophy.

Conclusions: Mechanical ventilation with PEEP results in longitudinal atrophy of diaphragm fibers, a response that is modulated by the elasticity of the giant sarcomeric protein titin. We postulate that longitudinal atrophy, in concert with the aforementioned cross-sectional atrophy, hampers spontaneous breathing trials in critically ill patients: during these efforts, end-expiratory lung volume is reduced, and the shortened diaphragm fibers are stretched to excessive sarcomere lengths. At these lengths, muscle fibers generate less force, and diaphragm weakness ensues.

Keywords: mechanical ventilation; PEEP; diaphragm; critically ill

(Received in original form September 23, 2017; accepted in final form March 26, 2018)

*These authors contributed equally.

Supported by NHLBI grant HL-121500 (C.A.C.O.), MSCA-RISE-2014 (Marie Skłodowska-Curie Actions – Research and Innovation Staff Exchange) grant 645648, and National Institute of Arthritis and Musculoskeletal and Skin Diseases grant R01AR053897 (H.G.).

Author Contributions: Study design: J.L., A.B., M.A.P., L.M.A.H., and C.A.C.O. Study coordination: J.L., M.v.d.B., L.M.A.H., and C.A.C.O. Patient inclusion: A.B., A.G., M.d.W., M.A.P., A.S.-d.M., and L.M.A.H. Biopsy obtaining: M.A.P. Data collection and analysis: J.L., M.v.d.B., and P.E.H. (biopsy handling and contractility experiments); J.L., M.v.d.B., P.E.H., R.v.d.P., C.v.d.B., J.S., and C.A.C.O. (animal experiments); J.L., S.B., J.K., and R.J.P.M. (stimulated emission depletion experiments); J.L., R.v.d.P., and S.S. (biochemical analysis); and J.E., Z.-H.S, and L.M.A.H. (patient diaphragm ultrasound). Data interpretation and analysis: J.L., M.v.d.B., P.E.H., A.B., M.A.P., H.G., L.M.A.H., and C.A.C.O. Drafting the article: J.L., M.v.d.B., L.M.A.H., and C.A.C.O. Figures: M.v.d.B., P.E.H., and C.A.C.O. Critical revision and final approval of the draft to be published: J.L., M.v.d.B., R.v.d.P., P.E.H., A.B., J.E., M.d.W., A.G., A.S.-d.M., Z.-H.S., C.v.d.B., S.B., S.S., J.S., H.G., J.K., R.J.P.M., M.A.P., L.M.A.H., and C.A.C.O.

Correspondence and requests for reprints should be addressed to Coen A. C. Ottenheijm, Ph.D., University of Arizona, Department of Cellular and Molecular Medicine, Medical Research Building, Room 322, 1656 E. Mabel Street, Tucson, AZ 85724. E-mail: coeno@email.arizona.edu.

This article has an online supplement, which is accessible from this issue's table of contents at www.atsjournals.org.

Am J Respir Crit Care Med Vol 198, Iss 4, pp 472–485, Aug 15, 2018

Originally Published in Press as DOI: 10.1164/rccm.201709-1917OC on March 26, 2018
Internet address: www.atsjournals.org

At a Glance Commentary

Scientific Knowledge on the Subject: Diaphragm weakness is highly prevalent in critically ill patients and contributes to weaning failure. The mechanisms underlying diaphragm weakness include reduced fiber thickness (i.e., cross-sectional atrophy) and impaired contractile function of the remaining fibers. Disuse is a recognized risk factor for critical illness–associated diaphragm weakness. However, the effects of positive end-expiratory pressure (PEEP) are unknown.

What This Study Adds to the Field: This study demonstrates that in critically ill patients, mechanical ventilation with PEEP results in reduced diaphragm fiber length due to a loss of contractile units in series (i.e., longitudinal atrophy). Consequently, diaphragm fibers are at a mechanical disadvantage when PEEP is released. In experimental models, we have identified specific molecular pathways, including titin-based mechanosensing, that are involved in the development of longitudinal atrophy.

Critically ill patients admitted to the intensive care unit rapidly develop diaphragm muscle weakness (1–6). Diaphragm weakness contributes to weaning failure and is associated with increased mortality rates (6–9). For establishing strategies to prevent or treat diaphragm weakness, a fundamental understanding of the underlying cellular mechanisms is crucial. Studies in mechanically ventilated brain dead organ donors suggest that reduced cross-sectional area of diaphragm fibers caused by activation of proteolytic pathways plays an important role (10–12). Using biopsy specimens from critically ill patients, we recently established that the contractility of individual diaphragm muscle fibers is severely impaired (13–15), partly accounted for by a reduced cross-sectional area of fibers (13). A mechanism that has been largely neglected is the effect of mechanical ventilation (MV) on diaphragm fiber length reduction, from here on referred to as longitudinal fiber atrophy (as opposed to the aforementioned cross-sectional fiber atrophy). Typically, critically ill patients are ventilated with positive end-expiratory pressure (PEEP) to limit alveolar collapse. However, PEEP-induced increase of end-expiratory lung volume may flatten the shape of the diaphragm dome, resulting in structural modifications in the diaphragm fibers.

We hypothesized that: *1*) the PEEP-induced increase in end-expiratory lung volume flattens the diaphragm dome and forces the muscle fibers to act at a shorter length during the respiratory cycle; *2*) the shorter fiber length causes structural adaptations in muscle fibers, either by loss of the number of sarcomeres (the smallest contractile units) in series to maintain optimal overlap of the myosin-based thick and actin-based thin filaments or by reducing the length of the thick and/or thin filaments; and *3*) diaphragm fiber length adaptations are modulated by titin, a giant protein that spans the length of the half sarcomere, forming a contiguous filament along the myofibril, and functions as a molecular spring that develops tension when sarcomere length changes. This layout of titin makes it ideally suited to sense changes in diaphragm length during MV with PEEP (16).

To test these hypotheses, we studied muscle fiber structure and contractility in diaphragm biopsies of mechanically ventilated critically ill patients and in mechanically ventilated rats with and without a mutation in the titin splice factor RNA binding motif 20 (*Rbm20*) that results in a more compliant titin molecule (17).

Methods

Additional details are in the online supplement.

Patients

Ultrasound. Ultrasound was performed in critically ill patients ($n = 15$; Table 1) with clinical indication for analysis of diaphragm function. M-mode ultrasound images were acquired while PEEP was acutely reduced with either 5 or 10 cm H_2O within one breath cycle. From the M-mode images obtained during subsequent breaths (Figure 1A), the caudal-cranial displacement of the diaphragm dome was calculated.

Biopsies. Diaphragm biopsies were obtained from mechanically ventilated critically ill patients undergoing abdominal or thoracic surgery for clinical indication (critically ill group; $n = 12$; Table 2). As a control group, diaphragm muscle biopsies were obtained from patients undergoing tumor removal of a suspected early-stage lung malignancy ($n = 12$, Table 3). Exclusion criteria are in the online supplement. The protocol was approved by the Medical Ethics Committee of the Vrije Universiteit Medical Center. Written informed consent was obtained from each patient and/or legal representative.

Biopsy handling, contractility of single fibers, and microscopy. These occurred as described in the online data supplement (13, 15, 18–26).

Rats

Long-term MV and contractility of intact diaphragm strips. Rats ($n = 12$) were mechanically ventilated for 18 hours. For details, *see* the online supplement (13, 27). To test the effect of titin-based mechanosensing on diaphragm remodeling, we used rats harboring a mutation in *Rbm20* causing expression of a giant titin isoform (17, 28). For details *see* the online supplement (29–32).

Acute effect of PEEP on diaphragm position. In a subset of ventilated rats, ultrasound was applied to visualize the effect of PEEP on diaphragm length. For details, *see* the online supplement.

Statistical Analyses

For details, *see* online supplement. Differences between groups were considered significant if $P < 0.05$.

Results

Patient Characteristics

Patient characteristics are shown in Tables 1–4. Pulmonary function data of control subjects are described in Table E1 in the online supplement.

Acute Effect of MV with PEEP on Diaphragm Position and Fiber Length in Critically ill Patients and Rats

To establish the acute effect of PEEP on the position of the diaphragm, we used

Table 1. General Characteristics of Critically Ill Patients on Whom Ultrasound Was Performed

Subject #	Age (*yr*)	Sex	BMI (kg/m^2)	Relevant Medical History	Reason for Admission to ICU	PEEP-induced Excursion (*cm*)	ΔPEEP (*cm* H_2O)	PEEP at Baseline (*cm* H_2O)	Support Pressure (*cm* H_2O)	V_T (*ml*)
1	63	F	19.1	COPD, pancreatitis	Pneumonia	0.204	5	5	18	371
2	67	F	29.4	AVNRT, polymyalgia rheumatica, adenectomy, lumpectomy	Septic arthritis	0.500	5	5	20	344
3	32	F	37.5	Tetraplegia	Sepsis, APL	0.147	5	14	12	483
4	57	M	23.4	None	OHCA	0.630	5	10	14	478
5	62	M	30.6	DM type II, CVA	Necrotizing fasciitis	0.534	5	10	4	595
6	70	M	25.2	COPD	OHCA	1.232	10	10	8	499
7	61	M	26.3	DM type II	*S. aureus* septic arthritis	1.073	10	10	12	583
8	67	F	27.3	Myelofibrosis, hypertension	ARDS	0.374	10	10	4	552
9	65	F	32.7	None	Multiple trauma (including thorax)	0.314	10	12	12	488
10	89	M	24.1	Benign prostatic hyperplasia; paroxysmal atrial fibrillation	Neurotrauma (including multiple rib fracture)	0.803	10	10	6	435
11	70	F	21.6	Multiple myeloma, DVT	Pneumonia	0.380	10	12	23	332
12	77	M	27.9	CABG, right upper lobectomy due to adenocarcinoma	IHCA during elective CAG	0.612	10	10	10	385
13	56	M	21.6	None	Intracranial hemorrhage	2.210	10	10	14	404
14	48	M	24.7	LBBB	OHCA	0.879	10	10	8	470
15	70	F	29.4	DM type II	Peritonitis	0.740	10	10	10	374

Definition of abbreviations: APL = acute promyeloid leukemia; ARDS = acute respiratory distress syndrome; AVNRT = atrioventricular nodal reentrant tachycardia; BMI = body mass index; CABG = coronary artery bypass graft; CAG = coronary angiography; COPD = chronic obstructive pulmonary disease; CVA = cerebrovascular accident; DM = diabetes mellitus; DVT = deep vein thrombosis; IHCA = in-hospital cardiac arrest; LBBB = left bundle branch block; OHCA = out-of-hospital cardiac arrest; PEEP = positive end-expiratory pressure; *S. aureus* = *Staphylococcus aureus*.

ultrasound to determine diaphragm displacement in critically ill patients caused by a decrease in PEEP (ΔPEEP) of 5 cm H_2O or 10 cm H_2O. Figure 1A (left and middle panels) shows typical B- and M-mode ultrasound images in which the cranial displacement of the diaphragm during ΔPEEP is visualized. Acute release of 5 cm H_2O PEEP caused a cranial diaphragm displacement in all five patients, with an average displacement of 0.40 ± 0.10 cm (Figure 1A, right panel). Acute ΔPEEP of 10 cm H_2O caused a cranial diaphragm displacement in all 10 patients, with an average displacement of 0.89 ± 0.17 cm (Figure 1A, right panel).

Investigating whether MV with PEEP, and the concomitant caudal movement of the diaphragm, shortens diaphragm fibers requires the isolation of whole-length (central tendon to rib cage) muscle fibers. This is impossible to establish in patients, as biopsies do not contain whole-length fibers, but it is feasible in rats. Thus, we first determined the effect of MV with PEEP (2, 3, and 5 cm H_2O) on diaphragm length in rats using ultrasonography. Figure 1B shows a typical B- (left) and M-mode (middle) ultrasound image, in which the acute effect of 3 cm H_2O PEEP is visualized in M-mode. Similar to patients, PEEP caused a caudal movement of the diaphragm (0.24 mm/cm H_2O; Figure 1B, right).

Next, we determined whether the caudal displacement shortens diaphragm fibers by perfusing rats with fixative immediately after the start of PEEP ventilation (2.5 cm H_2O) and during unassisted breathing (control). Arrest of diaphragm movement was complete within 10 seconds after start of fixation. At arrest of diaphragm movement, the phase of the respiratory cycle was not possible to determine, but on the basis of ultrasound observations in mice (33) we anticipate that arrest occurred at end-expiration. The *in vivo* fixated diaphragm was excised from the rats and whole-length (central tendon to rib cage) fibers were isolated from the midcostal region (note that diaphragm fibers were isolated from the same location in each rat; Figure 1C). The length of these fibers was significantly shorter in rats receiving PEEP ventilation (MV vs. control: 18.0 ± 0.5 vs. 19.9 ± 0.4 mm; Figure 1D), which was reflected by a reduced sarcomere length in the fibers (MV vs. control: 2.64 ± 0.06 vs. 2.85 ± 0.07 μm; Figure 1E). Thus, PEEP ventilation in rats results in a caudal displacement of the diaphragm, with a concomitant reduction of fiber and sarcomere length.

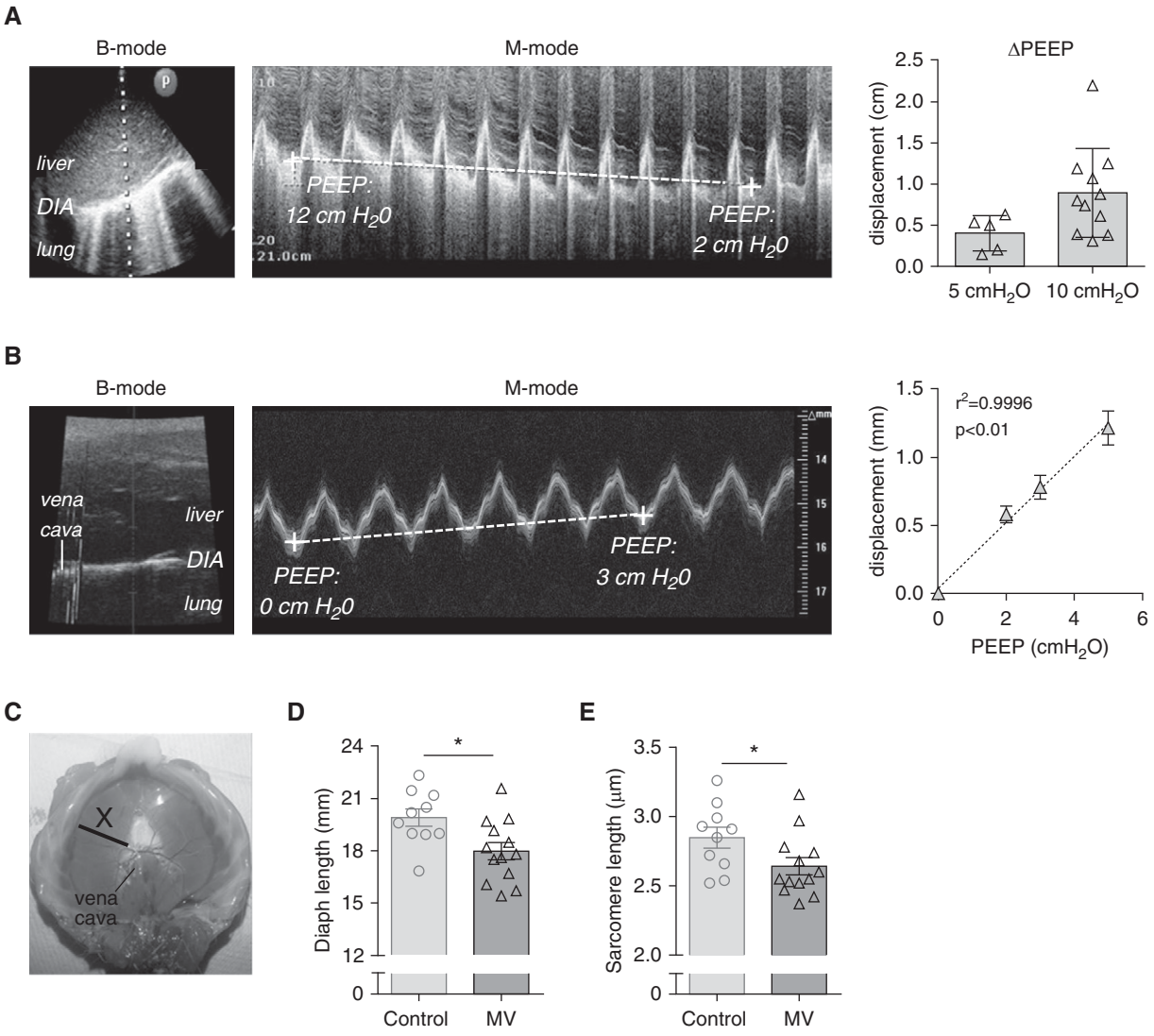

Figure 1. (*A*) Ultrasonographic view of the diaphragm (DIA) in a critically ill patient in the region of the liver dome, with B-mode image (left) and M-mode image (middle). The vertical dotted line in the left panel shows the location where the M-mode image was obtained, and P indicates the position of the probe. The M-mode image shows the acute effect of a 10 cm H_2O positive end-expiratory pressure (PEEP) change on the position of the DIA, measured at end-expiration (indicated by dashed line); note that in this patient PEEP was decreased from 12 to 2 cm H_2O, resulting in a cranial DIA displacement. Right: Cranial DIA displacement in critically ill patients caused by a 5 cm H_2O PEEP reduction ($n = 5$) or by a 10 cm H_2O PEEP reduction ($n = 10$); each data point is the average of three measurements per patient. (*B*) Ultrasonographic view of the DIA in rat during mechanical ventilation in the region of the liver dome is shown, with B-mode image (left) and corresponding M-mode image (middle). The vertical gray line shows the location where the M-mode image was obtained. The M-mode image shows that an increase of PEEP with 3 cm H_2O causes an acute caudal movement of the DIA, measured at end-expiration (dashed line). Right panel shows the effect of 2, 3, and 5 cm H_2O ΔPEEP on caudal DIA displacement; each data point is the average of five rats. (*C*) Image of an excised rat DIA, illustrating the midcostal position (X) where a strip was isolated for measurement of DIA fiber and sarcomere length in *in vivo*–fixated rats. (*D*) DIA fiber length in *in vivo*–fixated PEEP-ventilated (2.5 cm H_2O) rats and nonventilated rats; each data point represents one rat. (*E*) DIA sarcomere length in *in vivo*–fixated PEEP-ventilated (2.5 cm H_2O) rats and nonventilated rats; each data point represents one rat. Data in *A* and *B* show mean ± SD, and in *D* and *E* show mean ± SEM. *$P \leq 0.05$. Diaph = diaphragm; MV = mechanical ventilation.

Long-Term Effects of MV with PEEP on Diaphragm Fiber Length in Critically Ill Patients and Rats

Length adaptations in diaphragm fibers of critically ill patients. The average duration of MV in the critically ill patients before biopsy was 133 ± 38 hours (range, 17–435 h; Tables 3 and 4), and the average PEEP in the critically ill patients was 9.3 ± 1.0 cm H_2O (range, 6 ± 0.7 to 12 ± 1.7 cm H_2O; Table 4). To study whether PEEP and the concomitant shortening of the diaphragm induced length adaptations (i.e., structural changes in diaphragm fibers), we first applied a functional assay to determine thick and thin filament length in diaphragm fibers. Permeabilized individual muscle fibers were maximally activated at incremental sarcomere lengths, and the generated force was determined. Force at incremental sarcomere lengths was fitted using a second-order polynomial (19), which yielded three parameters that describe the force–sarcomere length relation: *1*) the sarcomere length at which maximum

Table 2. Characteristics of Critically Ill Patients from Whom Biopsies Were Obtained

Critically Ill Patient #	Age (*yr*)	Sex	BMI (kg/m^2)	Relevant Medical History	Reason of Admission to ICU	Surgery Where Biopsy Was Obtained	MV (*h*)	Septic	Died in ICU	APACHE II
1	47	F	22	None	Severe trauma	Relaparotomy: gauze removal	40	N	N	35
2	25	F	33	None	Severe trauma	Second relaparotomy: closure abdomen	219	Y	N	45
3	66	M	29	HT	Abdominal sepsis due to perforated appendicitis	Relaparotomy: rinsing abdominal cavity	28	Y	N	11
4	69	M	22	None	Esophageal rupture (Boerhaave syndrome)	Thoracotomy: esophageal repair	17	Y	N	27
5	51	M	29	Hypothyroidism	Severe trauma	Fourth relaparotomy: closure abdomen	85	N	N	30
6	72	M	20	T2DM, colon carcinoma, chronic bronchitis, COPD GOLD II	Abdominal sepsis due to duodenal perforation	Relaparotomy: cholecystectomy	20	Y	Y	19
7	74	M	25	HT, AFib	Respiratory failure due to bilateral pneumonia	Relaparotomy: evacuation empyema	435	Y	Y	19
8	22	F	20	None	Severe trauma	Second relaparotomy: closure abdomen	203	N	N	31
9	55	F	21	Lower leg amputation, right kidney infarction, splenic infarction	Abdominal sepsis due to perforations by intestinal ischemia	Relaparotomy: closure abdomen	69	Y	N	19
10	75	M	22	HT, chronic coronary artery disease, chronic kidney disease, smoker	Postoperative care after thoracoabdominal aortic aneurysm repair	Fourth relaparotomy: Hartmann procedure	290	Y	Y	22
11	54	M	26	None	Postoperative care after ruptured abdominal aortic aneurysm repair	Fourth relaparotomy: sigmoid resection with placement colostomy	50	N	N	40
12	66	F	21	Colitis	Severe trauma with intestinal damage	Fourth relaparotomy: rinsing abdominal cavity	134	Y	N	24

Definition of abbreviations: AFib = atrial fibrillation; APACHE = Acute Physiology and Chronic Health Evaluation; BMI = body mass index; COPD GOLD = chronic obstructive pulmonary disease (Global Initiative for Obstructive Lung Disease classification); HT = hypertension; MV = mechanical ventilation; T2DM = type 2 diabetes mellitus.

force is generated (SL_{opt}), *2*) the sarcomere length at which 50% of maximum force is generated (SL_{50}), and *3*) the sarcomere length at which the fit crosses the *x*-axis and thus no force is generated (SL_{max}; Figure 2A). Figure 2B shows that the average force–sarcomere length relation (with force normalized to its maximum) of the critically ill patients overlaps with that of the control patients. Figures 2C–2E show that SL_{opt}, SL_{50}, and SL_{max} are comparable between critically ill and control patients (critically ill vs. control, SL_{opt}: 2.66 ± 0.12 vs. 2.68 ± 0.12 μm; SL_{50}: 3.68 ± 0.11 vs. 3.70 ± 0.10 μm; SL_{max}: 4.10 ± 0.11 vs. 4.12 ± 0.12 μm). Thus, the sarcomere length–dependence of force is unaffected in muscle fibers of critically ill patients, suggesting that the length of the thin and thick filaments is not shortened.

Next, we directly measured the length of the thin and thick filaments. Thin and thick filament lengths were measured by stimulated emission depletion (STED) superresolution microscopy. An example of phalloidin-stained thin filaments is shown in Figure 3A. Average thin filament length was comparable between fibers of critically ill and control patients (critically ill vs. control: 1.28 ± 0.03 vs. 1.26 ± 0.05 μm). An example of myosin heavy chain–stained thick filaments is shown in Figure 3B. Average thick filament length was comparable between fibers of critically ill and control patients (critically ill vs. control: 1.79 ± 0.04 vs. 1.86 ± 0.03 μm). Thus, microscopy analyses confirm that thin and thick filament lengths are not shorter in diaphragm fibers of critically ill patients than in those of control patients. Determining the number of sarcomeres in series in the diaphragm of patients is not feasible (this would require biopsies spanning the length from central tendon to rib cage), and therefore we

Table 3. Characteristics of Control Patients

Control Patient #	Age (*yr*)	Sex	BMI (kg/m^2)	Relevant Medical History	TNM Classification	MV (*h*)
1	52	M	25	T2DM, HT, COPD GOLD II, ex-smoker	pT3N0M0	1.5
2	58	F	28	None	pT1aN0M0	2
3	56	M	21	COPD GOLD II, ex-smoker	pT4N2M0	2
4	60	F	26	HT	pT2aN0R0	0.75
5	59	F	28	Chronic bronchitis, smoker	Benign, cyst	0.75
6	64	F	26	COPD GOLD II, smoker	pT1bN0M0	1.25
7	64	M	31	HT, MI, T2DM, smoker	Benign, bronchiectasis and inflammation	1
8	55	F	27	Allergic asthma, recurrent pneumonia, smoker	Carcinoid T1bN0	1
9	40	M	24	None	Carcinoid pT1aN0R0	1.5
10	50	M	24	COPD GOLD I, smoker	Mucinous adenocarcinoma T1aN0M0	1.25
11	58	F	23	Chronic bronchitis, COPD GOLD I, ex-smoker	Adenocarcinoma pT0N0M0	2.5
12	69	M	33	HT, ex-smoker	Adenocarcinoma pT3N1M0	1.5

Definition of abbreviations: BMI = body mass index; COPD = chronic obstructive pulmonary disease (GOLD classification); GOLD = Global Initiative for Obstructive Lung Disease; HT = hypertension; MI = myocardial infarction; MV = mechanical ventilation; T2DM = type 2 diabetes mellitus; TNM = classification of tumors based on tumor size (T), lymph nodes involved (N), and metastases (M).

performed these studies in rats that were mechanically ventilated for 18 hours

Length adaptations in diaphragm fibers of 18-hour mechanically ventilated rats. Rats were mechanically ventilated for 18 hours with a PEEP of 2.5 cm H_2O. First, we validated the model and determined whether MV with PEEP had an effect on the contractile properties of the diaphragm. Midcostal diaphragm strips (isolated from the same location as for the determination of sarcomere length; Figure 1C) were isolated and electrically activated (schematic; Figure 4A). Similar to previous studies (34–37), maximal tension was decreased after 18 hours of MV (MV vs. control: 176 ± 12 vs. 278 ± 11 mN/mm^2; Figure 4B). Importantly, the diaphragm muscle strip length for maximal force production (optimal length, ML_{opt}; Figure 4A) was significantly reduced, by 12%, in ventilated rats (MV vs. control: 2.05 ± 0.36 vs. 2.33 ± 0.02 cm; Figure 4C). Thus, in rats, 18 hours of MV with PEEP causes contractile weakness, with the maximal force generated at a shorter muscle length.

Next, we determined whether the reduction of ML_{opt} was a reflection of a change in thick and/or thin filament length. Individual, permeabilized muscle fibers were maximally activated at incremental

Table 4. Specification of Duration and Settings of Mechanical Ventilation

Critically Ill Patient #	CMV (*h*)	AMV (*h*)	O_2 (*h*)	NR (*h*)	Total MV (*h*)	MV Mode before Obtaining Biopsy	FI_{O_2} (%)	PEEP ($cm\ H_2O$)	PEEP min–max ($cm\ H_2O$)	RR (*Breaths/min*)	V_T (*ml*)
1	40	0	0	0	40	PC (CMV)	47 ± 12	12 ± 0.9	7–14	23 ± 2	370 ± 71
2	128	91	0	0	219	PS/CPAP (AMV)	54 ± 20	15 ± 6.7	8–26	26 ± 4	392 ± 78
3	2	26	19	0	28	O_2 therapy	42 ± 11	5 ± 0.4	3–5	14 ± 4	762 ± 220
4	1	16	0	0	17	PC (AMV)*	57 ± 12	11 ± 1	10–12	23 ± 4	515 ± 170
5	85	0	0	0	85	SIMV + ASB (AMV)	44 ± 5	13 ± 2.1	8–15	22 ± 2	528 ± 102
6	12	8	1	0	20	CPAP + ASB (AMV)	50 ± 5	5 ± 0.4	5–6	21 ± 1	549 ± 38
7	275	160	152	0	435	SIMV + ASB (CMV)	47 ± 11	11 ± 3	5–15	18 ± 5	557 ± 143
8	92	111	0	0	203	PS/CPAP (AMV)	34 ± 8	8 ± 1.0	3–10	21 ± 5	337 ± 57
9	29	40	0	0	69	PC (CMV)	50 ± 10	8 ± 0.4	6–8	17 ± 7	584 ± 157
10	124	166	5	0	290	PC (CMV)	43 ± 4	7 ± 1.4	2–9	24 ± 5	526 ± 113
11	48	2	0	0	50	SIMV + ASB (CMV)	32 ± 2	12 ± 2.1	8–16	31 ± 1	494 ± 24
12	130	4	0	0	134	SIMV + ASB (CMV)	41 ± 7	5 ± 0.4	3–7	18 ± 2	400 ± 49

Definition of abbreviations: AMV = assisted mechanical ventilation; ASB = assisted spontaneous breathing; BIPAP = bi-level positive airway pressure; CMV = controlled mechanical ventilation; CPAP = continuous positive airway pressure; min–max = minimum–maximum; MMV = mandatory minute ventilation; MV = mechanical ventilation; NIV = noninvasive ventilation; NR = not registered (e.g., during transport of the patients or surgery); O_2 = oxygen therapy; PC = pressure control; PEEP = positive end-expiratory pressure; PS = pressure support; RR = respiratory rate; SIMV = synchronized intermittent mandatory ventilation; Total MV = sum of hours spent on MV from moment of intubation until biopsy; VC = volume control.
Data are totals or mean ± SD. Means and SD of FI_{O_2}, PEEP, RR, and V_T were calculated from hourly registration from moment of intubation until biopsy. CMV indicates mechanical ventilation in PC/VC/SIMV/MMV/BIPAP mode, and measured respiratory rate is lower or equal to set respiratory rate. AMV indicates mechanical ventilation in PS/CPAP/ASB/NIV mode, and ventilation in PC/VC/SIMV/MMV/BIPAP mode as the measured respiratory rate is higher than the set respiratory rate.
*Mechanical ventilation of critically ill patient #4 was set on PC ventilation but interpreted as AMV by us because the measured respiratory rate was higher than the set respiratory rate.

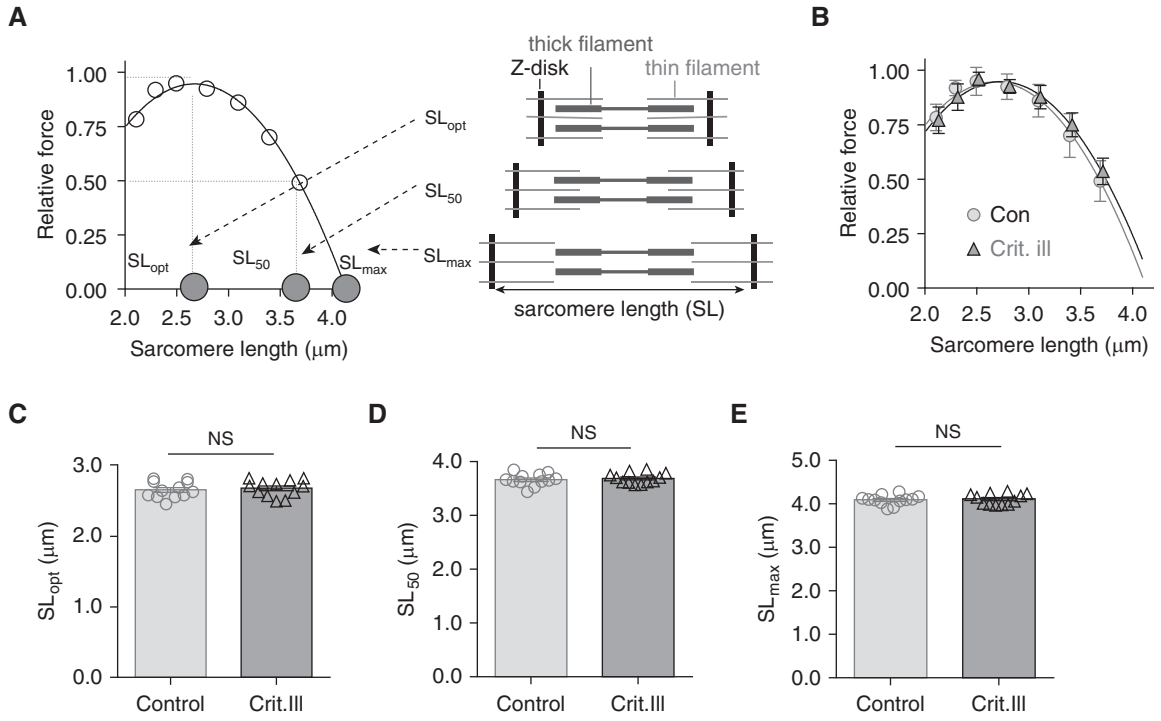

Figure 2. (*A*) Schematic showing the force–sarcomere length relation of a diaphragm fiber of a control patient; SL_{opt} is the sarcomere length at which maximal force is generated; SL_{50} is the sarcomere length at which 50% of maximal force is generated; SL_{max} is the sarcomere length at which no force is generated. Right panel shows schematics of a sarcomere with the corresponding lengths. (*B*) Force–sarcomere length relation of diaphragm fibers of 12 critically ill and 12 control patients are shown; note that both relations overlap. Force is presented as percentage of maximal force. (*C–E*) SL_{opt} (*C*), SL_{50} (*D*), and SL_{max} (*E*) are comparable between critically ill and control patients. Note that SL_{opt}, SL_{50}, and SL_{max} were not different between slow- and fast-twitch fibers (data not shown), and therefore these data are pooled. Also, in line with previous work (13–15), the maximal force-generating capacity was lower in both slow- and fast-twitch fibers of critically ill patients (data not shown). Each data point represents the average of ~10 fibers per subject. Data presented are mean ± SEM. Con = control patients; Crit.Ill = critically ill patients; NS = not significant.

sarcomere lengths. Figure 5A (top) shows that the average force–sarcomere length relation of fibers of the MV rats overlaps with that of fibers of control rats; SL_{opt} (Figure 5A, bottom), SL_{50}, and SL_{max} were comparable between MV and control rats (MV vs. control, SL_{opt}: 2.89 ± 0.41 vs. 2.81 ± 0.13 μm; SL_{50}: 3.69 ± 0.04 vs. 3.63 ± 0.03 μm; SL_{max}: 4.01 ± 0.05 vs. 3.97 ± 0.04 μm). To confirm that the length of the thin and thick filaments is not shorter in diaphragm fibers of the rats that received 18 hours MV, we measured thin and thickfilament length by STED superresolution microscopy. Examples of phalloidin-stained thin filaments and myosin heavy chain–stained thick filaments are shown in Figures 5B and 5C. Average thin-filament length (MV vs. control: 1.27 ± 0.02 vs. 1.29 ± 0.03 μm; Figure 5B) and average thick filament length (MV vs. control: 1.75 ± 0.02 vs. 1.74 ± 0.03 μm; Figure 5C) were comparable between fibers of MV and control rats. Thus, similar to the findings in critically ill patients, the length of the thin and thick filaments is not reduced in diaphragm fibers of rats that received 18 hours of MV with PEEP.

To determine whether the reduced ML_{opt} in MV rats was caused by a reduction in the number of sarcomeres in series, diaphragm fibers were isolated with the excised fibers spanning the whole distance from the central tendon to the ribs (Figure 1C, illustrated by line X). The length of these fibers was divided by the length of the sarcomeres, as determined by α-actinin staining (Figure 5D), to render the number of sarcomeres in series. Importantly, the number of sarcomeres in series was reduced by 12% in rats receiving MV compared with control animals (MV vs. control: 5,488 ± 128 vs. 6,250 ± 170 sarcomeres; Figure 5E). Thus, 18 hours of MV with PEEP causes longitudinal atrophy of diaphragm muscle fibers due to absorption of sarcomeres in series.

Effect of Compliant Titin on Diaphragm Fiber Length Remodeling during MV

We tested the hypothesis that low titin stiffness, by preconditioning the diaphragm to reduced titin-based mechanosensing, blunts the longitudinal atrophy response during diaphragm shortening caused by MV with PEEP. We studied rats with a mutation in the titin splicing factor *Rbm20* (17, 28), resulting in a more compliant titin molecule (the sarcomeric location of titin is shown in Figure 6A). As shown in Figure 6B, diaphragm fibers of Rbm20-deficient rats express a titin isoform that is larger than in fibers of wild-type (wt) rats. By coelectrophoresing diaphragm samples of wt or Rbm20-deficient rats with titin isoforms of known sizes (*see* Methods) we estimated that the difference in titin isoform size is ~110 kD. To verify that this larger isoform results in lower titin-based passive tension, individual diaphragm fibers were passively stretched: Figure 6C shows that, as

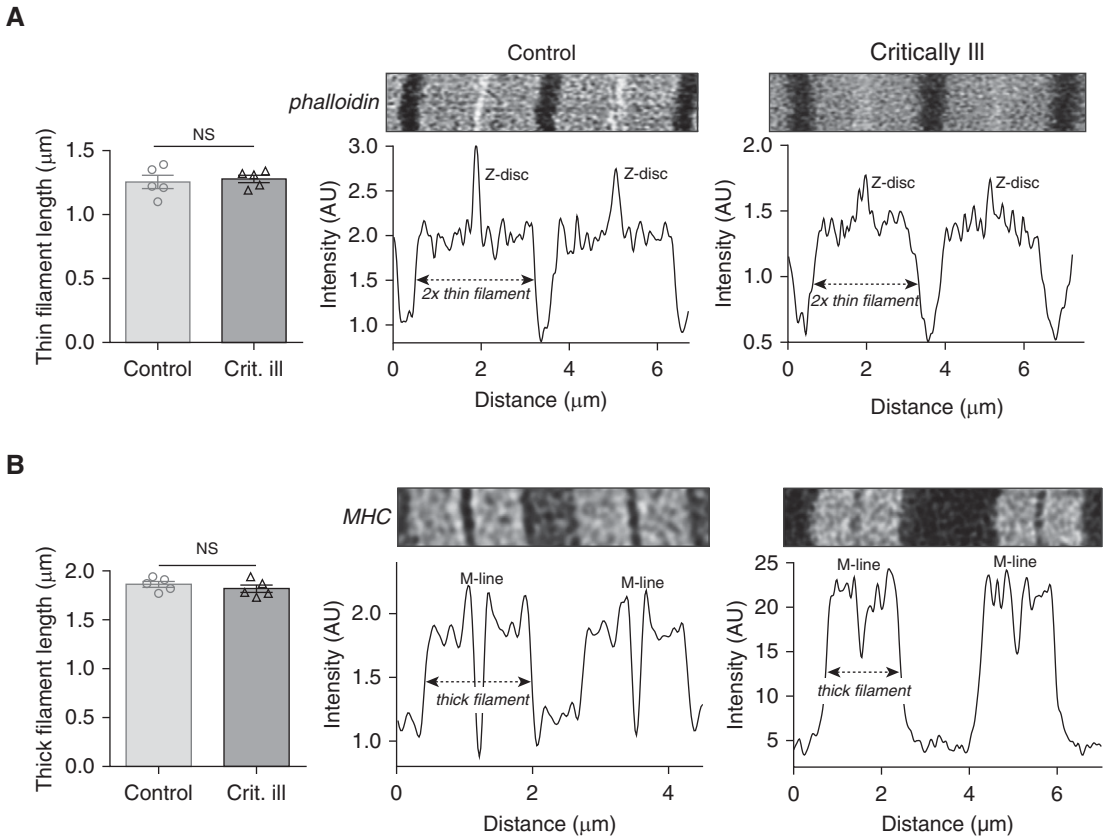

Figure 3. (*A*) Deconvolved stimulated emission depletion (STED) superresolution microscopy images of sarcomeres in a diaphragm fiber of a control and a critically ill patient, labeled with AlexaFluor-conjugated phalloidin to visualize the thin filaments. Intensity measurements were used to determine thin filament length, which was comparable between critically ill and control patients. (*B*) Deconvolved STED superresolution microscopy images of sarcomeres in a diaphragm fiber of a control and a critically ill patient, labeled with MHC (myosin heavy chain) antibodies to visualize the thick filaments, are shown. Intensity measurements were used to determine thick filament length, which was comparable between critically ill and control patients. Note that each data point represents the average of 50 to 100 sarcomeres per subject. Data presented are mean ± SEM. AU = arbitrary units; Crit. ill = critically ill patient; NS = not significant.

expected, fibers of Rbm20-deficient rats generate lower passive tension than fibers from wt rats. Subsequently, these rats were mechanically ventilated with 2.5 cm H_2O PEEP for 18 hours. Midcostal diaphragm strips were isolated and electrically activated. Maximal tension was reduced after 18 hours MV (298 ± 13 vs. 189 ± 9 mN/mm^2, control vs. MV, respectively), but this decrease was less pronounced in rats with the compliant titin isoform (241 ± 7 vs. 215 ± 7 mN/mm^2, control vs. MV, respectively; tension decrease after MV, wt vs. Rbm20-def: 37 ± 3% vs. 11 ± 3%; $P <$ 0.001; Figure 6D). Furthermore, the ML_{opt} of diaphragm strips from wt rats was reduced after MV (2.39 ± 0.02 vs. 2.03 ± 0.07 cm, control vs. MV, respectively), and this reduction was smaller and not significant in Rbm20-deficient rats that had received MV (2.24 ± 0.06 vs. 2.22 ± 0.10 cm, control vs. MV, respectively; ML_{opt} decrease after MV, wt vs. Rbm20-def: 15 ± 3% vs. 1 ± 4%; Figure 6E). Finally, the number of sarcomeres in series was not significantly reduced by 18 hours of MV in the Rbm20-deficient rats (7,155 ± 173 vs. 7,005 ± 317, control vs. MV, respectively; $P = 0.69$; Figure 6F), whereas this reduction was significant in wt rats (6,255 ± 170 vs. 5,488 ± 117, control vs. MV, respectively; sarcomere number decrease after MV, wt vs. Rbm20-def: 12 ± 2% vs. 2 ± 4%).

Thus, these results suggest that titin is involved in diaphragm fiber length remodeling during MV with PEEP.

Discussion

Our findings show that *1*) MV with PEEP causes a caudal movement of the diaphragm dome, both in critically ill patients and in rats. Additional studies in rats reveal that this caudal movement of the diaphragm reduces fiber and sarcomere length; *2*) diaphragm fibers adapt to the reduced length by absorbing sarcomeres in series, with no changes in thick or thin filament length in both rats and critically ill patients; *3*) titin's elastic properties modulate this length adaptation.

Longitudinal Atrophy of Diaphragm Fibers

PEEP is applied in nearly all mechanically ventilated critically ill patients to mitigate alveolar collapse, thereby improving oxygenation and respiratory mechanics. However, application of PEEP is associated with adverse effects in some patients due to alveolar overdistention and hemodynamic compromise. The present study provides strong evidence that PEEP may have adverse effects on diaphragm function as well. In particular, PEEP causes

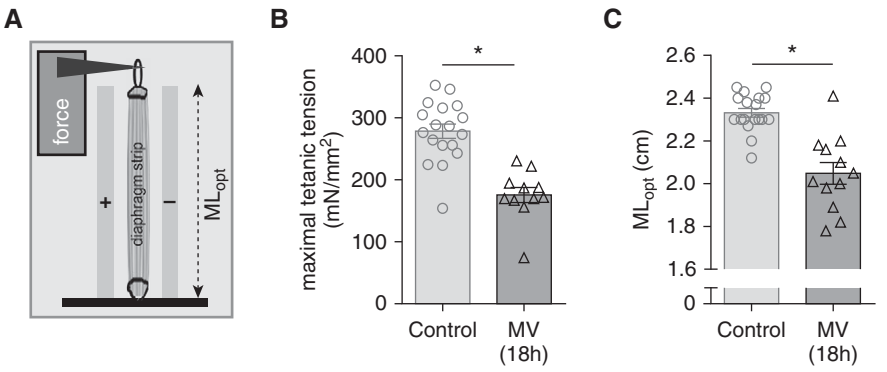

Figure 4. *In vitro* contractility of electrically stimulated diaphragm strips of 18-hour mechanically ventilated (MV) rats. (*A*) Schematic showing a full-length diaphragm strip in the experimental setup. The strips were isolated from the midcostal region, similar to location X in Figure 1C. ML_{opt} is the strip length at which maximal force is generated. (*B*) The maximal tension (force normalized to the cross-sectional area of the strip) was significantly lower in rats that were MV for 18 hours. (*C*) ML_{opt} was significantly shorter in the rats that were MV for 18 hours. Note that each data point represents one rat. Data presented are mean ± SEM. $^*P \leq 0.05$.

a caudal movement of the diaphragm dome, with a shortening of the zone of apposition (Figure 1). This shortening leads to structural adaptions in muscle fibers, as indicated by the reduced length at which diaphragm fibers generate maximal force after 18 hours of MV (Figure 4C). Such reduction had been suggested in previous studies (37) but remained controversial (38). This controversy is at least partly due to difficulties in the exact determination of optimal muscle length: determination of where muscle fibers end and the tendon starts with the naked eye is prone to error. Therefore, to obtain conclusive evidence for fiber shortening during MV with PEEP, we used microscopy analyses to measure the number of sarcomeres in series in whole-length diaphragm fibers in rats and found this number to be decreased (Figure 5). The magnitude of the decrease completely accounts for the reduction of optimal length (both 12%; Figures 4C and 5E). Thus, the present study is the first to show that MV with PEEP causes not only cross-sectional fiber atrophy but also longitudinal fiber atrophy (i.e., reduced length of fibers). Although adaptations might occur more rapidly in rats than in humans, we speculate that the rapid time course of longitudinal atrophy in the diaphragm fibers of rats suggests that this mechanism contributes to the rapid development, within 24 hours (9), of *in vivo* diaphragm weakness in critically ill patients. In these studies (9), transdiaphragmatic twitch pressure was determined at the end of expiration and at zero PEEP, thus with the length of the diaphragm fibers on the descending limb of the force–length relation.

Disuse of skeletal muscle causes reduction of the length of the myosin-based thick filaments (39), but such reduction was not observed in diaphragm fibers of mechanically ventilated critically ill patients or in ventilated rats. To rule out that length changes were too small to detect, we determined thick and thin filament length by STED superresolution microscopy. STED superresolution microscopy creates non–diffraction-limited images by the selective deactivation of fluorophores, minimizing the area of illumination at the focal point and thus enhancing the achievable resolution (40). Accordingly, thick filament measurements in the present study had a precision of ∼50 nm and thin filament measurements of ∼90 nm, a precision required for detection of small yet relevant differences in length. We anticipate that the duration of disuse in the rats (18 h) may have been too short to cause filament length changes in the diaphragm. Furthermore, although the patients were on MV much longer than the rats, diaphragm activity was not completely absent in the majority of critically ill patients but varied depending on the ventilation mode, respiratory drive, level of sedation, and the use of neuromuscular blocking agents (Table 4). It is likely that even these low levels of diaphragm activity are sufficient to attenuate changes in filament length.

Role for the Giant Muscle Protein Titin?

Our studies into the mechanisms that underlie the longitudinal atrophy of diaphragm fibers during MV with PEEP suggest a role for the giant elastic protein titin. Titin is the largest protein known to date and spans the entire length of the sarcomere from Z-disk to M-band (Figure 6A). The central I-band region of titin is extensible and functions as a spring that generates passive tension when the sarcomere is stretched. Titin filaments overlap in both the Z-disk and M-band, forming a contiguous filament along the myofibril. This layout of titin within the muscle's sarcomere makes it ideally suited to sense length changes. Indeed, titin links mechanical stress sensing to trophic signaling pathways via several titin-binding proteins (16). We hypothesized that low titin stiffness—by preconditioning the diaphragm to reduced mechanosensing—blunts the longitudinal atrophy response during diaphragm shortening caused by MV with PEEP. To test this hypothesis, we took advantage of Rbm20-deficient rats that have reduced titin-based stiffness (17, 28). Long-term MV of mice is technically challenging, and the availability of this mutant rat model provided us with the unique opportunity to overcome this limitation. The rat model carries a homozygous mutation in the titin splice factor *Rbm20*, leading to the expression of a diaphragm titin isoform that is ∼110 kD larger than in wt rats, with a concomitant reduction in titin-based passive stiffness of diaphragm fibers (Figure 6C: at end-expiratory sarcomere length [∼2.85 μm, Figure 1E] passive tension is ∼30% lower in Rbm20-deficent rats). The data support our hypothesis: after 18 hours of MV with PEEP, the development of diaphragm weakness is attenuated in the Rbm20-deficient rats (Figure 6D) and, importantly, the optimal length for force generation and the number of sarcomeres in series in diaphragm fibers of ventilated Rbm20-deficient

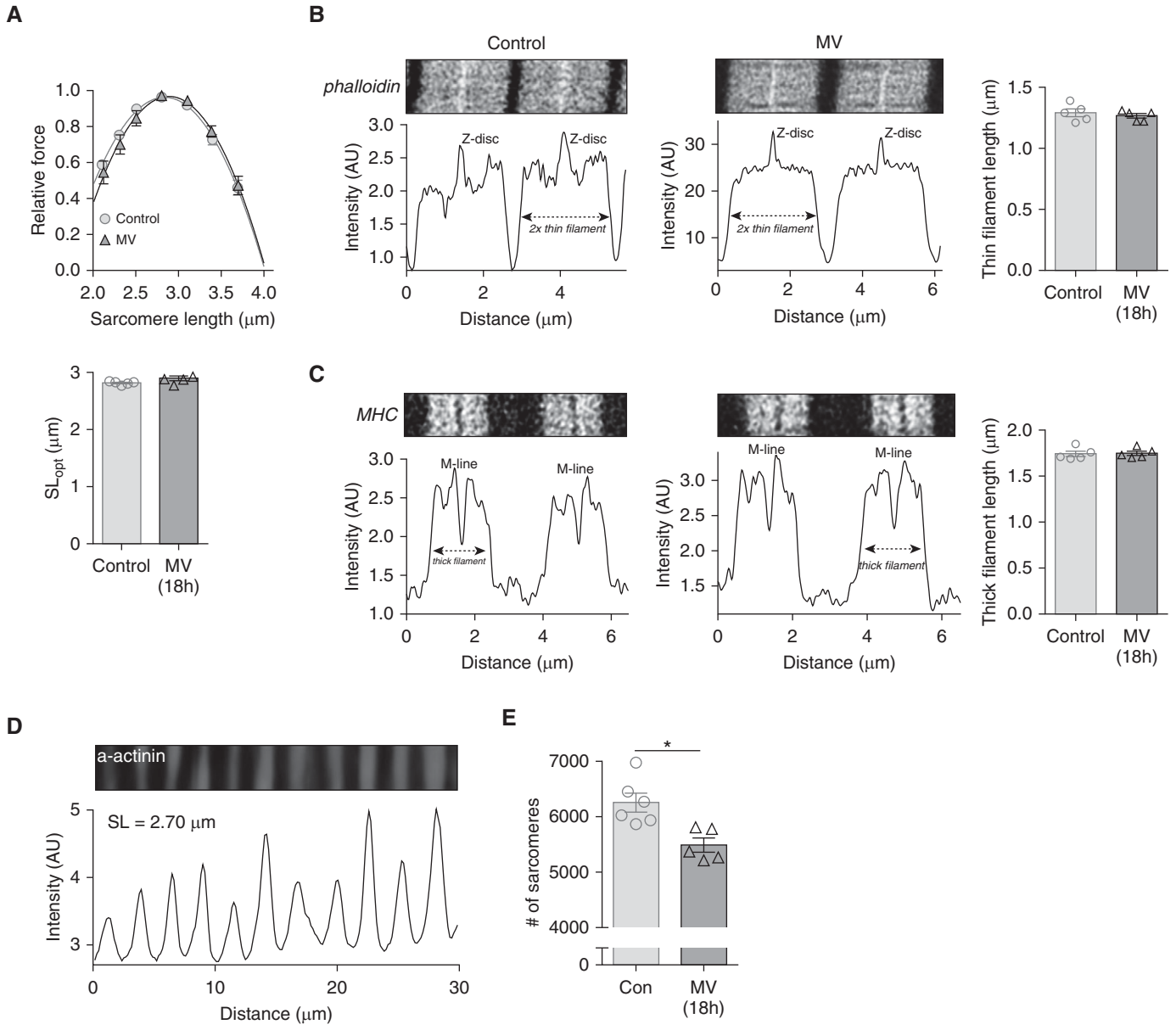

Figure 5. (*A*) Top: Force–sarcomere length relation of diaphragm fibers of 18-hour mechanically ventilated (MV) rats and control rats; note that both relations overlap. Force is presented as percentage of maximal force; each data point is the average of five rats. Bottom: SL_{opt} is comparable between MV and control rats. Note that ~90% of fibers were fast-twitch, and therefore both fiber types were pooled. In line with previous work (32, 50), the maximal force-generating capacity was lower in fibers of MV rats (data not shown). (*B*) Deconvolved stimulated emission depletion (STED) superresolution microscopy images of sarcomeres in a diaphragm fiber of a control and an 18-hour MV rat, labeled with AlexaFluor-conjugated phalloidin to visualize the thin filaments. Intensity measurements were used to determine thin filament length, which was comparable between 18-hour MV and control rats. Each data point represents one rat. (*C*) Deconvolved STED superresolution microscopy images of sarcomeres in a diaphragm fiber of a control and an 18-hour MV rat, labeled with MHC (myosin heavy chain) antibodies to visualize the thick filaments. Intensity measurements were used to determine thick filament length, which was comparable between 18-hour MV and control rats. Each data point represents one rat. (*D*) Typical α-actinin staining in a rat diaphragm fiber to visualize the Z-discs to determine sarcomere length. (*E*) The number of sarcomeres in series is significantly lower in 18-hour MV rats than in control rats. Each data point represents the average of one rat; 2,000 to 3,000 sarcomeres were measured per rat. Data presented are mean ± SEM. *$P \leq 0.05$. AU = arbitrary units; Con = control; SL = sarcomere length; SL_{opt} = sarcomere length at which maximal force is generated.

rats are not significantly different from nonventilated Rbm20-deficient rats (Figures 6E and 6F). These findings support the concept in which titin-based mechanosensing modulates the length adaptation of diaphragm fibers during MV with PEEP. Future studies should unravel the titin-based signaling pathways that underlie this effect.

Study Limitations

First, for the measurement of diaphragm displacement during PEEP variation, ultrasound was used. In each patient and rat, the ultrasound probe was placed at the same

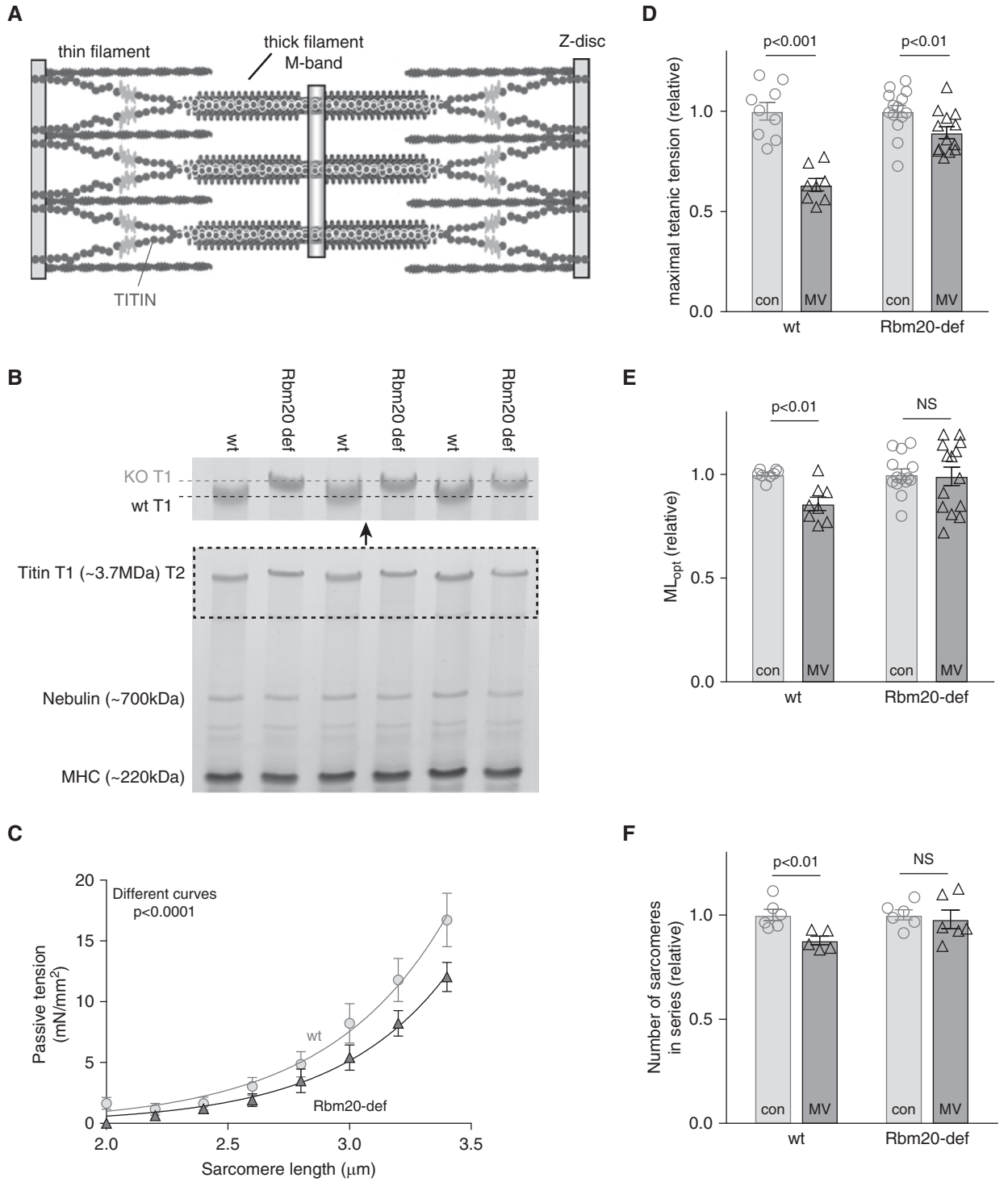

Figure 6. (*A*) Schematic of the layout of the giant protein titin in the muscle sarcomere. (*B*) Bottom: 1% sodium dodecyl sulfate–agarose gel illustrating the slower mobility of the larger titin isoform in the RNA binding motif 20 (Rbm20)-deficient rats. T1 is full-length titin, T2 is a titin degradation product. Top: Magnification of T1 titin; note the lower titin mobility in Rbm20-deficient rats. (*C*) Passive tension–sarcomere length relation in diaphragm fibers. Note that the larger titin isoform in Rbm20-deficient rats results in lower passive tension (each data point represents the average of six rats). (*D*) Eighteen hours of mechanical ventilation causes significant contractile weakness of intact diaphragm strips in control rats. The development of this weakness is blunted in 18-hour mechanically ventilated Rbm20-deficient rats. (*E*) The strip length at which maximal force is generated (ML_{opt}) is reduced in 18-hour mechanically ventilated control rats, but this reduction is absent in Rbm20-deficient rats. (*F*) The number of sarcomeres in series is not significantly reduced in 18-hour mechanically ventilated Rbm20-deficient rats compared with nonventilated Rbm20-deficient rats. Each data point represents one rat; 2,000 to 3,000 sarcomeres were measured per rat. Data presented are mean ± SEM. con = control; KO = knockout; MHC = myosin heavy chain; MV = mechanical ventilation; NS = not significant; Rbm20-def = RNA binding motif 20–deficient; wt = wild type.

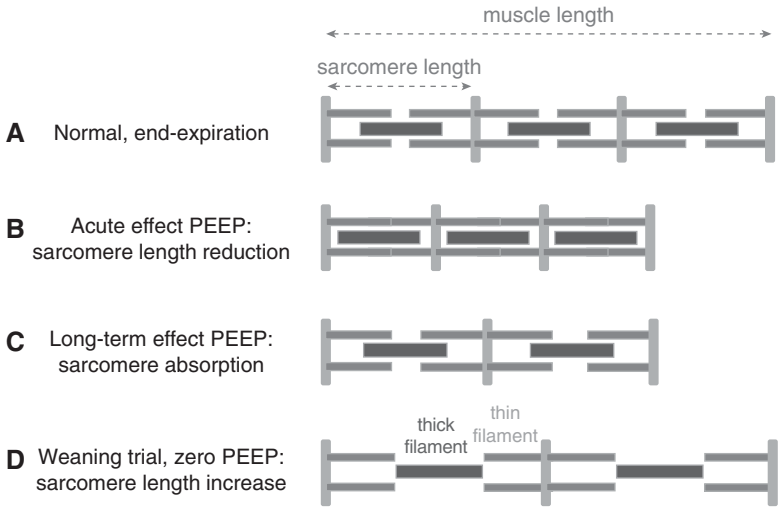

Figure 7. Schematic illustrating the development of longitudinal atrophy in diaphragm fibers during mechanical ventilation with positive end-expiratory pressure (PEEP). (*A*) Muscle length in a spontaneous breathing rat at end-expiration. For simplicity, only three sarcomeres are drawn. (*B*) The acute effect of PEEP on sarcomere length. (*C*) Long-term PEEP causes sarcomere absorption to restore sarcomere length. (*D*) During weaning and normalization of end-expiratory pressure, the diaphragm fibers are stretched to lengths beyond optimal sarcomere length. The schematic shows a length at which thick–thin filament overlap is absent and no force can be generated by the muscle fiber.

position and approximately the same region of the diaphragm was imaged. However, because two-dimensional images were obtained, we cannot rule out that the magnitude of displacement was different in other regions of the diaphragm.

Second, we did not include a group of rats that were ventilated with zero PEEP, and therefore we cannot rule out that the observed longitudinal atrophy of diaphragm fibers is the result of MV *per se*, whether or not PEEP is applied. However, ventilation with zero PEEP might cause atelectasis and an (systemic) inflammatory response (41, 42), which in turn might impair diaphragm fiber structure and function, thereby confounding the results. Furthermore, it is highly unlikely that ventilation with zero PEEP induces longitudinal atrophy: this type of atrophy (i.e., sarcomere in series absorption), only occurs when muscles are put at shorter (sarcomere) length (43). Our ultrasound data show a strong correlation between PEEP and caudal diaphragm movement (Figure 1B), a movement that was associated with sarcomere shortening (Figure 1E). The rats in the present study were on controlled mechanical ventilation, and it is unknown whether complete inactivity of the diaphragm affects fiber length or aggravates the effects of PEEP. However, in rats with joint immobilization, so that muscle length was fixed at normal operational length, denervation (i.e., lack of muscle activity) does not induce sarcomere absorption, whereas denervation of the same muscle but fixed at a shorter length does promote longitudinal fiber atrophy (44). Taken together, this supports a concept in which PEEP-induced diaphragm shortening is the main factor contributing to longitudinal atrophy of diaphragm fibers during MV.

Third, we postulate that the force–length relation of the diaphragm is affected by sarcomere absorption, but this postulation assumes that the mechanical characteristics of the central tendon and of the tissues that connect the diaphragm muscle to the costae are unaffected. In theory, lengthening of the central tendon would allow the shorter fibers to operate at the plateau region of the force–length relation, thereby mitigating the effects of longitudinal fiber atrophy. However, long-term shortening of lower limb muscle is associated with a decrease in tendon length, an adaptation that would aggravate (not mitigate) the effects of longitudinal fiber atrophy (for review see Reference 45).

Clinical Implications

The findings of the current study point toward a novel mechanism for failing a spontaneous breathing trial in patients weaning from MV. The acute reduction or withdrawal of PEEP decreases end-expiratory lung volume and thereby stretches the adapted, short diaphragm fibers to long sarcomere lengths. This will force the muscle fibers to operate on the disadvantageous descending limb of the force–length relation, where overlap of the thick and thin filaments is suboptimal, and thus contribute to diaphragm weakness (for schematic, see Figure 7). This longitudinal atrophy of fibers adds to the contractile weakness caused by ultrastructural damage and cross-sectional fiber atrophy (34, 46). The magnitude of this contribution depends on the level of applied PEEP: assuming that in rats before the application of MV with PEEP the sarcomere length in the diaphragm is ~2.85 μm at end-expiration (Figure 1E) and that 12% of sarcomeres are absorbed during 18-hour MV with 2.5 cm H_2O PEEP (Figure 5E), after removal of MV with PEEP at similar diaphragm fiber length the sarcomere length would be ~3.24 μm (2.85/0.88) at end-expiration, thus already at the descending limb of the force–length relation (Figure 5A). Considering that 2.5 cm H_2O PEEP in rats is estimated to correspond to 5 to 6 cm H_2O PEEP in humans (estimation based on respiratory system compliance of 64 ml/cm H_2O and TLC of 5,167 ml for humans [47] versus 0.51 ml/cm H_2O and TLC of 16.7 ml for rats [48, 49]), the nearly twofold higher average PEEP in our cohort of patients (Table 4) may have significant detrimental effect on the operating sarcomere length in the diaphragm (note that PEEP levels in patients varied, but that the average lowest PEEP level [i.e., $PEEP_{min}$ in Table 4], was 6.0 ± 0.7 cm H_2O, a level comparable to that in the ventilated rats). We postulate that this longitudinal diaphragm atrophy contributes to difficulties with weaning patients from MV, especially in patients who have respiratory disease or preexisting diaphragm weakness. Our findings suggest that slow reduction in PEEP is advisable, to allow for the reversal of longitudinal atrophy. Clearly, this reasoning should be tested in future studies. ■

Author disclosures are available with the text of this article at www.atsjournals.org.

References

1. Watson AC, Hughes PD, Louise Harris M, Hart N, Ware RJ, Wendon J, *et al*. Measurement of twitch transdiaphragmatic, esophageal, and endotracheal tube pressure with bilateral anterolateral magnetic phrenic nerve stimulation in patients in the intensive care unit. *Crit Care Med* 2001;29:1325–1331.
2. Hermans G, Agten A, Testelmans D, Decramer M, Gayan-Ramirez G. Increased duration of mechanical ventilation is associated with decreased diaphragmatic force: a prospective observational study. *Crit Care* 2010;14:R127.
3. Jaber S, Petrof BJ, Jung B, Chanques G, Berthet JP, Rabuel C, *et al*. Rapidly progressive diaphragmatic weakness and injury during mechanical ventilation in humans. *Am J Respir Crit Care Med* 2011; 183:364–371.
4. Gottesman E, McCool FD. Ultrasound evaluation of the paralyzed diaphragm. *Am J Respir Crit Care Med* 1997;155:1570–1574.
5. Goligher EC, Fan E, Herridge MS, Murray A, Vorona S, Brace D, *et al*. Evolution of diaphragm thickness during mechanical ventilation. impact of inspiratory effort. *Am J Respir Crit Care Med* 2015;192: 1080–1088.
6. Dres M, Dubé BP, Mayaux J, Delemazure J, Reuter D, Brochard L, *et al*. Coexistence and impact of limb muscle and diaphragm weakness at time of liberation from mechanical ventilation in medical intensive care unit patients. *Am J Respir Crit Care Med* 2017;195:57–66.
7. Esteban A, Anzueto A, Frutos F, Alía I, Brochard L, Stewart TE, *et al*.; Mechanical Ventilation International Study Group. Characteristics and outcomes in adult patients receiving mechanical ventilation: a 28-day international study. *JAMA* 2002;287:345–355.
8. Supinski GS, Callahan LA. Diaphragm weakness in mechanically ventilated critically ill patients. *Crit Care* 2013;17:R120.
9. Demoule A, Jung B, Prodanovic H, Molinari N, Chanques G, Coirault C, *et al*. Diaphragm dysfunction on admission to the intensive care unit: prevalence, risk factors, and prognostic impact-a prospective study. *Am J Respir Crit Care Med* 2013;188:213–219.
10. Levine S, Nguyen T, Taylor N, Friscia ME, Budak MT, Rothenberg P, *et al*. Rapid disuse atrophy of diaphragm fibers in mechanically ventilated humans. *N Engl J Med* 2008;358:1327–1335.
11. Hussain SN, Mofarrahi M, Sigala I, Kim HC, Vassilakopoulos T, Maltais F, *et al*. Mechanical ventilation-induced diaphragm disuse in humans triggers autophagy. *Am J Respir Crit Care Med* 2010;182:1377–1386.
12. Picard M, Jung B, Liang F, Azuelos I, Hussain S, Goldberg P, *et al*. Mitochondrial dysfunction and lipid accumulation in the human diaphragm during mechanical ventilation. *Am J Respir Crit Care Med* 2012;186:1140–1149.
13. Hooijman PE, Beishuizen A, Witt CC, de Waard MC, Girbes AR, Spoelstra-de Man AM, *et al*. Diaphragm muscle fiber weakness and ubiquitin-proteasome activation in critically ill patients. *Am J Respir Crit Care Med* 2015;191:1126–1138.
14. van den Berg M, Hooijman PE, Beishuizen A, de Waard MC, Paul MA, Hartemink KJ, *et al*. Diaphragm atrophy and weakness in the absence of mitochondrial dysfunction in the critically ill. *Am J Respir Crit Care Med* 2017;196:1544–1558.
15. Hooijman PE, Beishuizen A, de Waard MC, de Man FS, Vermeijden JW, Steenvoorde P, *et al*. Diaphragm fiber strength is reduced in critically ill patients and restored by a troponin activator. *Am J Respir Crit Care Med* 2014;189:863–865.
16. Ottenheijm CA, van Hees HW, Heunks LM, Granzier H. Titin-based mechanosensing and signaling: role in diaphragm atrophy during unloading? *Am J Physiol Lung Cell Mol Physiol* 2011;300:L161–L166.
17. Guo W, Schafer S, Greaser ML, Radke MH, Liss M, Govindarajan T, *et al*. RBM20, a gene for hereditary cardiomyopathy, regulates titin splicing. *Nat Med* 2012;18:766–773.
18. Ottenheijm CA, Hooijman P, DeChene ET, Stienen GJ, Beggs AH, Granzier H. Altered myofilament function depresses force generation in patients with nebulin-based nemaline myopathy (NEM2). *J Struct Biol* 2010;170:334–343.
19. Ottenheijm CA, Hidalgo C, Rost K, Gotthardt M, Granzier H. Altered contractility of skeletal muscle in mice deficient in titin's M-band region. *J Mol Biol* 2009;393:10–26.
20. de Man FS, van Hees HW, Handoko ML, Niessen HW, Schalij I, Humbert M, *et al*. Diaphragm muscle fiber weakness in pulmonary hypertension. *Am J Respir Crit Care Med* 2011;183:1411–1418.
21. Manders E, Ruiter G, Bogaard HJ, Stienen GJ, Vonk-Noordegraaf A, de Man FS, *et al*. Quadriceps muscle fibre dysfunction in patients with pulmonary arterial hypertension. *Eur Respir J* 2015;45:1737–1740.
22. Lawlor MW, Ottenheijm CA, Lehtokari VL, Cho K, Pelin K, Wallgren-Pettersson C, *et al*. Novel mutations in NEB cause abnormal nebulin expression and markedly impaired muscle force generation in severe nemaline myopathy. *Skelet Muscle* 2011;1:23.
23. Ottenheijm CA, Lawlor MW, Stienen GJ, Granzier H, Beggs AH. Changes in cross-bridge cycling underlie muscle weakness in patients with tropomyosin 3-based myopathy. *Hum Mol Genet* 2011; 20:2015–2025.
24. Ottenheijm CA, Witt CC, Stienen GJ, Labeit S, Beggs AH, Granzier H. Thin filament length dysregulation contributes to muscle weakness in nemaline myopathy patients with nebulin deficiency. *Hum Mol Genet* 2009;18:2359–2369.
25. Ottenheijm CA, Buck D, de Winter JM, Ferrara C, Piroddi N, Tesi C, *et al*. Deleting exon 55 from the nebulin gene induces severe muscle weakness in a mouse model for nemaline myopathy. *Brain* 2013;136:1718–1731.
26. Winter JM, Joureau B, Lee EJ, Kiss B, Yuen M, Gupta VA, *et al*. Mutation-specific effects on thin filament length in thin filament myopathy. *Ann Neurol* 2016;79:959–969.
27. Manders E, de Man FS, Handoko ML, Westerhof N, van Hees HW, Stienen GJ, *et al*. Diaphragm weakness in pulmonary arterial hypertension: role of sarcomeric dysfunction. *Am J Physiol Lung Cell Mol Physiol* 2012;303:L1070–L1078.
28. Greaser ML, Warren CM, Esbona K, Guo W, Duan Y, Parrish AM, *et al*. Mutation that dramatically alters rat titin isoform expression and cardiomyocyte passive tension. *J Mol Cell Cardiol* 2008;44:983–991.
29. Warren CM, Krzesinski PR, Greaser ML. Vertical agarose gel electrophoresis and electroblotting of high-molecular-weight proteins. *Electrophoresis* 2003;24:1695–1702.
30. Granzier HL, Irving TC. Passive tension in cardiac muscle: contribution of collagen, titin, microtubules, and intermediate filaments. *Biophys J* 1995;68:1027–1044.
31. Ottenheijm CA, Knottnerus AM, Buck D, Luo X, Greer K, Hoying A, *et al*. Tuning passive mechanics through differential splicing of titin during skeletal muscle development. *Biophys J* 2009;97:2277–2286.
32. van Hees HW, Schellekens WJ, Andrade Acuña GL, Linkels M, Hafmans T, Ottenheijm CA, *et al*. Titin and diaphragm dysfunction in mechanically ventilated rats. *Intensive Care Med* 2012;38:702–709.
33. Van der Pijl R, Strom J, Conijn S, Lindqvist J, Labeit S, Granzier H, *et al*. Titin-based mechanosensing modulates muscle hypertrophy. *J Cachexia Sarcopenia Muscle* [online ahead of print] 5 Jul 2018; DOI: 10.1002/jcsm.12319.
34. Shanely RA, Zergeroglu MA, Lennon SL, Sugiura T, Yimlamai T, Enns D, *et al*. Mechanical ventilation-induced diaphragmatic atrophy is associated with oxidative injury and increased proteolytic activity. *Am J Respir Crit Care Med* 2002;166:1369–1374.
35. Le Bourdelles G, Viires N, Boczkowski J, Seta N, Pavlovic D, Aubier M. Effects of mechanical ventilation on diaphragmatic contractile properties in rats. *Am J Respir Crit Care Med* 1994;149:1539–1544.
36. Sassoon CS, Caiozzo VJ, Manka A, Sieck GC. Altered diaphragm contractile properties with controlled mechanical ventilation. *J Appl Physiol (1985)* 2002;92:2585–2595.
37. Yang L, Luo J, Bourdon J, Lin MC, Gottfried SB, Petrof BJ. Controlled mechanical ventilation leads to remodeling of the rat diaphragm. *Am J Respir Crit Care Med* 2002;166:1135–1140.
38. Sassoon CS, Zhu E, Fang L, Sieck GC, Powers SK. Positive end-expiratory airway pressure does not aggravate ventilator-induced diaphragmatic dysfunction in rabbits. *Crit Care* 2014;18:494.
39. Udaka J, Ohmori S, Terui T, Ohtsuki I, Ishiwata S, Kurihara S, *et al*. Disuse-induced preferential loss of the giant protein titin depresses muscle performance via abnormal sarcomeric organization. *J Gen Physiol* 2008;131:33–41.
40. Dyba M, Jakobs S, Hell SW. Immunofluorescence stimulated emission depletion microscopy. *Nat Biotechnol* 2003;21:1303–1304.
41. Vreugdenhil HA, Heijnen CJ, Plötz FB, Zijlstra J, Jansen NJ, Haitsma JJ, *et al*. Mechanical ventilation of healthy rats suppresses peripheral immune function. *Eur Respir J* 2004;23:122–128.

42. Chu EK, Whitehead T, Slutsky AS. Effects of cyclic opening and closing at low- and high-volume ventilation on bronchoalveolar lavage cytokines. *Crit Care Med* 2004;32:168–174.
43. Williams PE, Goldspink G. The effect of immobilization on the longitudinal growth of striated muscle fibres. *J Anat* 1973;116:45–55.
44. Goldspink G, Tabary C, Tabary JC, Tardieu C, Tardieu G. Effect of denervation on the adaptation of sarcomere number and muscle extensibility to the functional length of the muscle. *J Physiol* 1974; 236:733–742.
45. Harvey LA, Herbert RD. Muscle stretching for treatment and prevention of contracture in people with spinal cord injury. *Spinal Cord* 2002;40:1–9.
46. Bernard N, Matecki S, Py G, Lopez S, Mercier J, Capdevila X. Effects of prolonged mechanical ventilation on respiratory muscle ultrastructure and mitochondrial respiration in rabbits. *Intensive Care Med* 2003;29:111–118.
47. Henderson WR, Chen L, Amato MBP, Brochard LJ. Fifty years of research in ARDS: respiratory mechanics in acute respiratory distress syndrome. *Am J Respir Crit Care Med* 2017;196: 822–833.
48. Rubini A, El-Mazloum D, Morra F, Bosco G. The effect of body cooling on respiratory system mechanics and hysteresis in rats. *Respir Physiol Neurobiol* 2013;189:52–58.
49. Bolle I, Eder G, Takenaka S, Ganguly K, Karrasch S, Zeller C, *et al*. Postnatal lung function in the developing rat. *J Appl Physiol (1985)* 2008;104:1167–1176.
50. Schellekens WJ, van Hees HW, Kox M, Linkels M, Acuña GL, Dekhuijzen PN, *et al*. Hypercapnia attenuates ventilator-induced diaphragm atrophy and modulates dysfunction. *Crit Care* 2014;18: R28.